Comparison of Experimental Surface and Flow Field Measurements to Computational Results of the Juncture Flow Model

Nettie H. Roozeboom,[1]
NASA Ames Research Center, Moffett Field, CA 94035

Henry C. Lee,[2]
Science and Technology Corp., Moffett Field, CA 94035

Laura J. Simurda,[3] Gregory G. Zilliac,[4] and Thomas H. Pulliam[5]
NASA Ames Research Center, Moffett Field, CA 94035

Wing-body juncture flow fields on commercial aircraft configurations are challenging to compute accurately. The NASA Advanced Air Vehicle Program's juncture flow committee is designing an experiment to provide data to improve Computational Fluid Dynamics (CFD) modeling in the juncture flow region. Preliminary design of the model was done using CFD, yet CFD tends to overpredict the separation in the juncture flow region. Risk reduction wind tunnel tests were requisitioned by the committee to obtain a better understanding of the flow characteristics of the designed models. NASA Ames Research Center's Fluid Mechanics Lab performed one of the risk reduction tests. The results of one case, accompanied by CFD simulations, are presented in this paper. Experimental results suggest the wall mounted wind tunnel model produces a thicker boundary layer on the fuselage than the CFD predictions, resulting in a larger wing horseshoe vortex suppressing the side of body separation in the juncture flow region. Compared to experimental results, CFD predicts a thinner boundary layer on the fuselage generates a weaker wing horseshoe vortex resulting in a larger side of body separation.

I. Introduction

THE NASA Transformational Tools and Technologies Project (TTT), under the Advanced Air Vehicle Program, is sponsoring a substantial effort to further investigate the origin of separation bubbles found in wing-body juncture zones. A multi-year effort with several large-scale wind tunnel tests is planned.[1] Six wing configurations were designed using Computational Fluid Dynamics (CFD) methods, and risk reduction tests have been and will be conducted to help better understand these configurations within the context of the juncture flow committee design requirements. NASA Ames Research Center's Fluid Mechanics Lab (FML) performed one of the low-cost risk reduction tests to help guide the Juncture Flow (JF) committee in planning future large-scale wind tunnel tests. The nature of this work was originally intended to be a risk assessment experiment, to obtain a quick look at the several designs being proposed for the larger JF effort. As will be seen, the correlation between the CFD and the FML experiment results is not as strong as the correlation between the results from the CFD and a later test performed at Virginia Tech.[1] This spurred an exploration of some of the differences observed between computation and experiment. Further details on the JF experiment and the additional risk-reduction experiments can be found in an accompanying paper by Rumsey *et al*.[1]

CFD was used extensively in designing the candidate geometries. Because the models were designed with CFD, the primary goal of the experiment was to gather data demonstrating the CFD-designed models had the desired flow features commonly seen in wing-body junctions. The experiments conducted at Ames and Virginia Tech[1] were thus designed to be low cost and to provide the JF community with a first look at experimental data.

---

[1] Aerospace Engineer, Experimental Aero-Physics Branch, M.S. 260-1, AIAA Member.
[2] Research Scientist/Engineer, Computational Aerosciences Branch, M.S. 258-2, AIAA Member
[3] Aerospace Engineer, Experimental Aero-Physics Branch, M.S. 260-1, AIAA Member
[4] Research Scientist, Experimental Aero-Physics Branch, M.S. 260-1, AIAA Member
[5] Senior Research Scientist, Computational Aerosciences Branch, M.S. 258-2, AIAA Member

The FML tests investigated both surface and off-surface flow features in and around the wing-body junction. Two wing designs were investigated – the F6v2 (the conventional DRL F6 wing[2]) and the F6-S12 (symmetrized DRL-F6 merged with a NACA 00xx seraies, see Rumsey *et al*.[1]). These separate wings were mounted in succession on the semi-span Juncture Flow Model (JFM) fuselage. The cost of the model for this experiment was less than $25K for the fuselage and two different wings (F6v2, F6S12) with and without a horn.

Boundary layer surveys, skin friction measurement, and oil flow visualizations were collected and compared to CFD results. Boundary layer surveys were taken at the inlet, upstream of the leading edge junction and along the wing-body junction to understand the development and characteristics of the boundary layer. Fringe Imaging Skin Friction (FISF) was used to determine the surface skin friction magnitude and direction.[5] Oil flow visualizations were performed to characterize the wing-body flow field. Results of these measurements are compared with Reynolds Averaged Navier Stokes simulations. Of the several model configurations studied over a range of angles of attack, the F6v2 model (with wing leading edge horn) at zero angle of attack and Reynolds number of 0.62 million was selected for investigation in this paper. Results presented will be limited to the boundary layer surveys and oil flow visualizations.

II. Background

A concerted international effort is underway to improve computational simulation techniques to the point where they can be reliably used to predict aircraft drag to within a few drag counts. This effort, being led by the AIAA Applied Aerodynamics Technical Committee under the moniker "Drag Prediction Workshop (DPW)" with open participation by industry, academia and government labs, has been very productive in identifying the deficiencies in computational modeling and developing validation cases that are leading to improved computational fidelity. A side benefit of this effort has been a reexamination of the accuracy and uncertainity of the "tried and true" approaches to wind tunnel testing that have been motivated by the ever diminishing differences between simulation and experiment. Flow features that were previously "in the noise" are now significant; however, it is important to note that not all errors are produced by the CFD modeling - it is equally valid to question the accuracy of the measured result as it is the computation.

In the Drag Prediction Workshops 3 to 5, a wide range of side-of-body separation bubble sizes were reported across many different CFD codes. The bubble size varied greatly with many factors, including grid resolution, grid topology, and numerical schemes.[3] The introduction of the quadratic constitutive relation (QCR) made the predicted separation bubble size over various CFD codes more homogenous.[4] QCR modifies the Reynold's stresses aligning them with the flow, and improving the corner flow CFD predictions. However, the separation bubble size as measured in wind tunnel tests still did not agree with CFD predictions, even with QCR applied. It is suspected that deficiencies in turbulence modeling are leading to these discrepancies, but there is insufficient measured surface and flow field data characterizing the separation zones to draw a conclusion.

It is not surprising that the wing-fuselage juncture flow is challenging to compute accurately because, in this region, the turbulent boundary layers on the fuselage and wing merge together to produce a horseshoe vortex embedded in a flow that undergoes the adverse pressure gradient created by the wing geometry as the trailing edge is approached on the wing suction side. To further complicate matters, the off-surface juncture flow has been observed by many to be highly three dimensional. In addition, the wing surface skin friction level decreases as the trailing edge is approached.[5] So it should be expected that the trailing edge junction is a very sensitive region within the flow field and therefore is difficult to both compute and measure accurately.

The most comprehensive review survey of the juncture flow in the literature was produced by Simpson.[6] This survey looked at many different types of juncture flows, including blunt and streamlined flows, and found that they are characterized by flow three dimensionality and unsteadiness. The review elucidated the importance of accurately capturing seemingly subtle geometrical effects such as corner radii.

Gand *et al.*[7] also studied the wing juncture flow field both experimentally and numerically. They found that the horseshoe vortex meanders (i.e. is unsteady) in their large eddy simulations (LES) of the wing juncture2 flow. The horseshoe vortex was seen to exhibit bi-modal behavior, which can be problematic in obtaining repeatable time-averaged measurements and challenging to compute using Reynolds averaged Navier Stokes codes. Furthermore, the turbulent Reynolds stresses were highly anisotropic in the corner. CFD simulations that utilize turbulence models, wherein the stress is modeled as isotropic (i.e. the majority of one and two equation models commonly used), should not be expected to produce satisfactory results. Gand *et al*. suggest stress anisotropy is the primary cause of poor RANS computational accuracy in previous studies.

III. Procedure

Experimental Technique

Experimental data were collected in the NASA Ames Fluid Mechanics Lab's (FML's) 32×48 inch open circuit, in-draft wind tunnel with a sonic throat. As shown in figure 1 below, the air enters the bell-mouth, passes through a honeycomb structure and 3 screens, and then passes into a 9:1 contraction. Downstream of the contraction is the test section, which is 48 inches wide, 32 inches tall and 120 inches long. The facility centrifugal compressor runs at constant speed and mass flow through the test section is controlled by a variable-area sonic throat downstream of the test section. The free-stream turbulence intensity was previously measured as 0.15% of the freestream velocity (documented flat-plate transition Reynolds number of 2 million) and the core flow angularity is less than 0.3 deg. This facility is commonly referred to as Test Cell 2 or TC2.

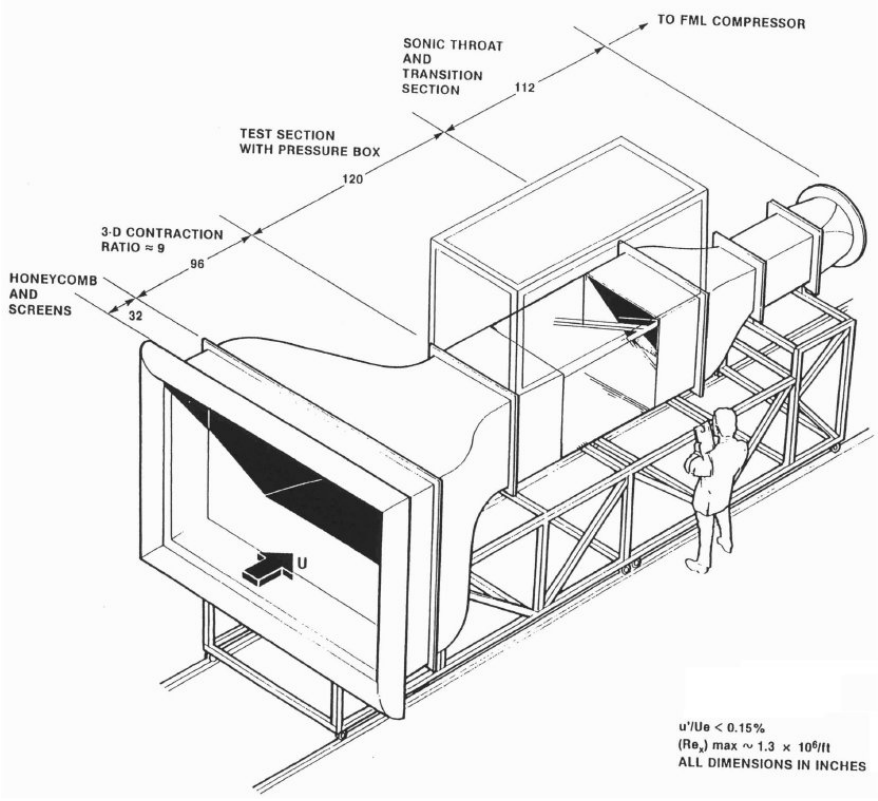

Figure 1. Model of NASA Ames Fluid Mechanics Lab 32×48 inch wind tunnel.

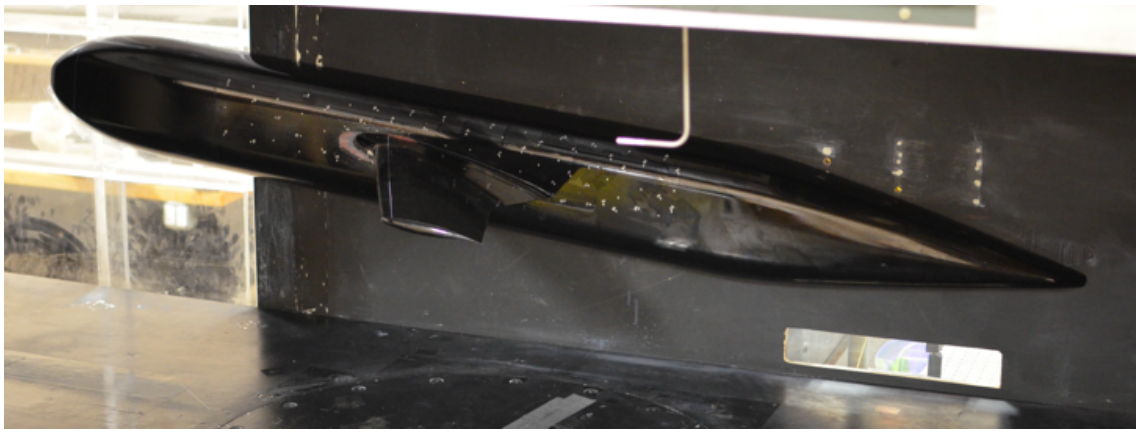

Figure 2. Three percent scaled semi-span juncture flow model wall-mounted in TC2.

A 3%-scaled semi-span model was chosen for this experiment (see figure 2). The fuselage was manufactured from inexpensive and easy to machine polyurethane based modeling board. The wing and a section of the fuselage were machined from the same billet of 6061 aluminum. The wing was designed with an integral root to keep the wing-body junction uniform and repeatable after multiple installations. As shown in the computer aided drawing (CAD) models in figure 3, the wing plus junction was attached to a mounting plate. Several mounting plates were machined for the various incidence angles (0˚, 2˚, 4˚, 6˚ and 8˚), permitting accurate and repeatable incidence angle setting as shown in figure 3.

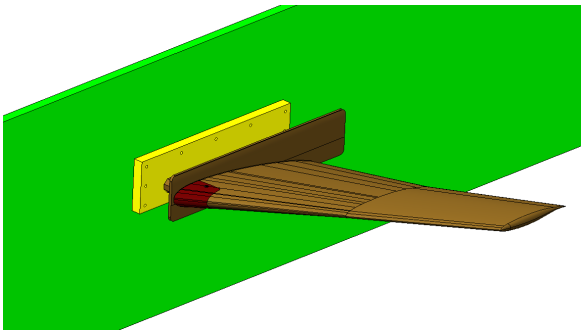

Figure 3. CAD Model showing wing and mounting plate.

The TC2 tunnel coordinate system is shown in figure 4. *X* runs the length of the tunnel, *Z* is up, and *Y* is towards the model. (0,0,0) is located at the center of the inlet plane. Units are in inches.

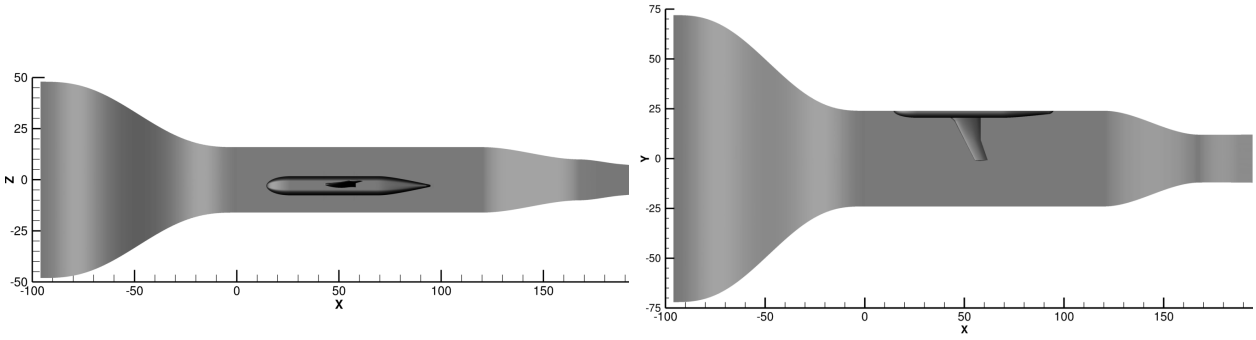

Figure 4. Side and top views of TC2 (*X, Y, Z* axes and coordinates are shown in inches).

An MKS Instruments 698A Barotron differential pressure transducer was used to measure the tunnel reference total and static pressure. Two pitot-static probes are mounted on a traversing stage on the ceiling of the test section. The tunnel velocity was computed from the dynamic pressure obtained from these pitot static probes.

The boundary layer measurements were collected using a conical 0.025 inch diameter United Sensors total pressure probe (model BA-025-12-C-11-650). This probe was connected to a recently calibrated MKS Instruments 223BD differential pressure transducer. The static pressure from the pitot static probe was measured at the same tunnel station location as the boundary layer measurement. The probe was held by a 0.75 inch diameter probe stem extension attached to a three-axis traverse system with incremental positioning accuracy of better than 0.001 inch.

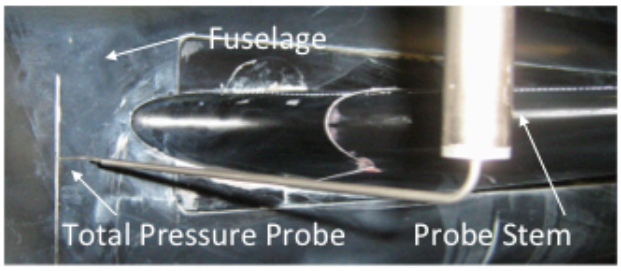

Figure 5. Total pressure boundary layer probe installation.

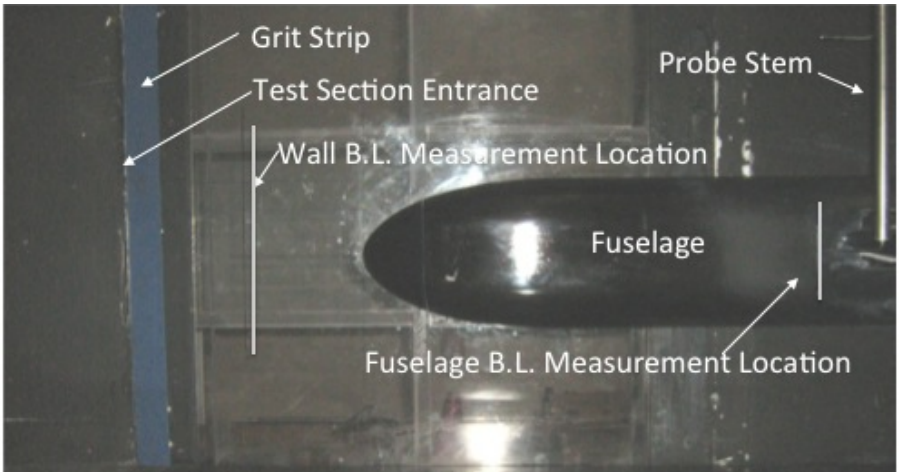

Figure 6. Side wall and Location of Total Pressure Probe.

Numerous boundary layers surveys were obtained using a total pressure probe. Boundary layer measurements were acquired upstream of the fuselage (midway between the start of the test section and the nose of the fuselage at $X = 7.75$ inch) and at locations along the fuselage side wall and on the wing suction side surface as shown in Figures 5-8. The figures also show where 3 profiles were recorded upstream of the wing leading edge at $X = 41.625$ inch. Because the junction was the area of interest, 4 stations above the wing were investigated at $X = 45.75$ inch, 49.75 inch, 53.75 inch, and 56.25 inch.

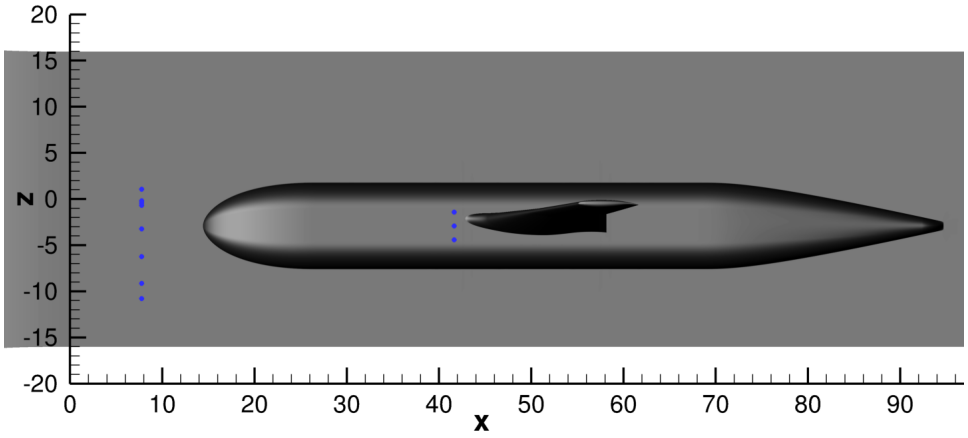

Figure 7. Boundary layer survey locations on fuselage.

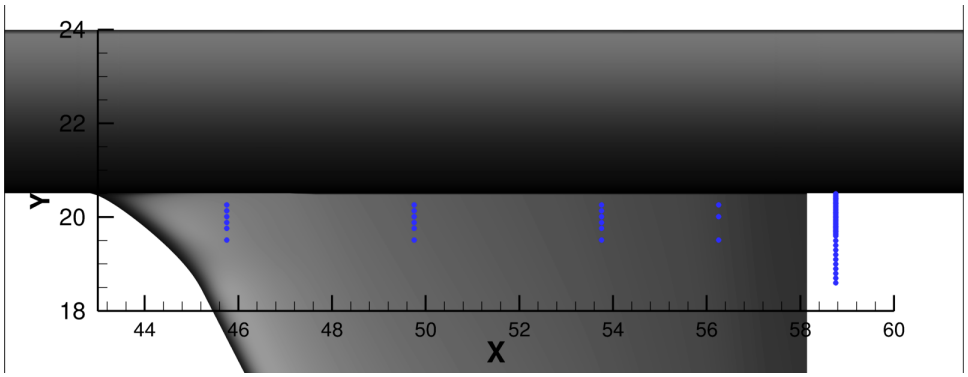

Figure 8. Boundary layer survey locations on wing and in the wake.

Because a conical total pressure probe was used for the boundary layer measurements, CFD was used to investigate flow angularity. This proves important. If the angle between the probe axis and the incoming flow is too large, the probe will not accurately measure the total pressure and the measurements from the probe need to be adjusted. For the probe used, the total pressure will be within 1% of the actual total pressure for flow angles up to approximately 15-20˚. The CFD results, as shown in figure 9, indicate the vast majority of boundary layer data are not significantly impacted by the flow angle. However, in data measured downstream of the trailing edge, where the flow angle becomes appreciable, the measured velocity will be less than the actual velocity in the wind tunnel.

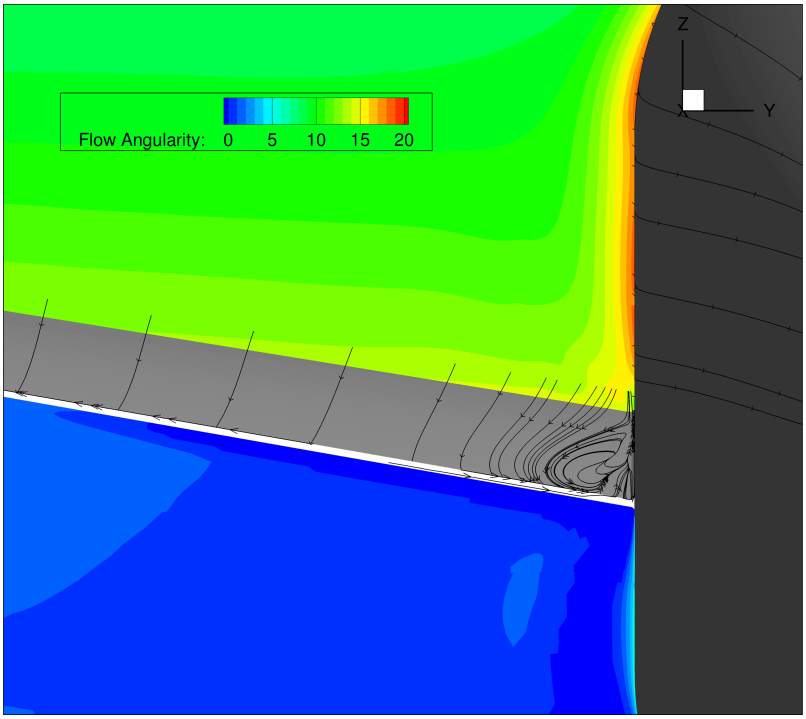

Figure 9. CFD result at X = 56.25 inch, showing contours of flow angularity.

In order to further validate the test results, several repeat test runs were carried out to demonstrate the repeatability of boundary layer data. Figure 10 below shows quite reasonable repeatability for the runs of three boundary layer profiles taken on the fuselage.

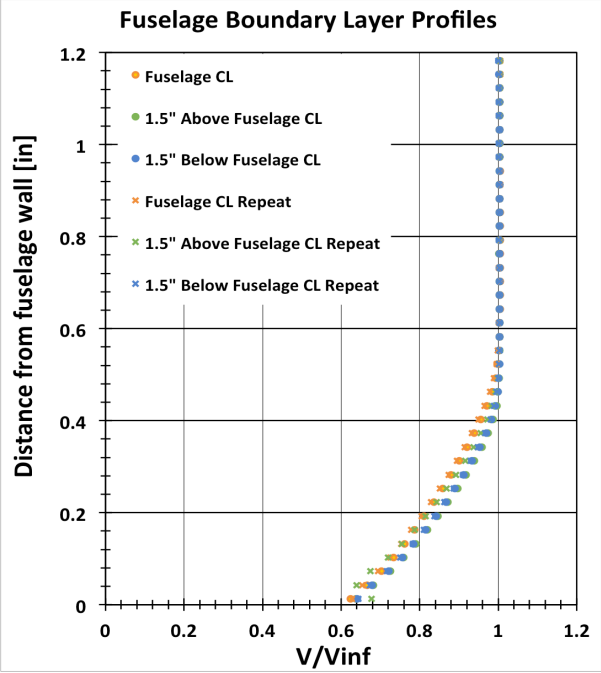

Figure 10. Repeatability of boundary layer survey on the fuselage, X = 41.625 inch.

Computational Technique

CFD simulations were performed in conjunction with the experiment in TC2. While lower fidelity simulations (free-air, simplified tunnel) were used initially to model the TC2 geometry, these results were ruled out because the uncertainty caused by the simplifications, had not been quantified nor validated. Thus, a full model of the TC2 tunnel geometry, including the inlet contraction section, the test section, and the exit contraction, was used to model the physical experiment as closely as possible. Furthermore, the exit contraction section was extended linearly to model the sonic throat. The final area of the throat was obtained through one-dimensional isentropic relations. The CFD grids were built in accordance to the best practices as outlined in the AIAA drag prediction workshop series.[7]

Overflow 2.2k, a Reynolds averaged Navier-Stokes code was used for the CFD analysis.[8] The Roe upwind scheme along with the ARC3D diagonalized Beam-Warming scalar pentadiagonal scheme were used. Full multigrid cycles were used to help initialize the solution and help accelerate the convergence. Solutions were run in the steady-state mode. The Spalart-Almaras turbulence model with the rotational correction and QCR were used.[4,10,11] The nozzle inflow boundary condition, where total temperature and total pressure are specified, was used at the inlet. A specified pressure outflow boundary condition was applied at the tunnel exit. The exit (back) pressure was varied until the test section speed matched the experiment.

All the simulations were performed on Pleiades, one of the supercomputers at NASA Ames Research Center. Pleiades is an SGI Ice cluster with 189,000 cores (combination of Haswell, Ivy Bridge, Sandy Bridge, and Westmere Xeon Processors). Cases were typically run with 1200-1400 cores, depending on computing resource availability, for typically 12-24 hours. Simulations were typically run 50,000-100,000 steps until convergence was achieved.

The JFM-F6v2 with horn grids were created with a combination of both Ansa 15.3 and Chimera Grid Tools (CGT).[11] The same CAD outer mold line (OML) used to manufacture the model was used. Ansa was used for geometry cleanup and to produce a watertight triangularization. The CGT software package was used to create a set of overset grids. The JFM-F6v2 vehicle was modeled with 9 grid zones including 3 for the fuselage and 6 for the wing, resulting in a total of 24.8 million grid points. The TC2 tunnel was modeled using 9 grid zones, including 6 grids modeling all of the tunnel walls (two per inlet, test section, and exit), and three core grids, resulting in a total of 127.7 million grid points. The wall grids were combined with the F6 grids to produce the final setup. All the surface and volume grids were built with a growth rate of 1.15 and a y+ of less than 1.0. Figures 11 and 12 show the F6 grid topology as installed in TC2.

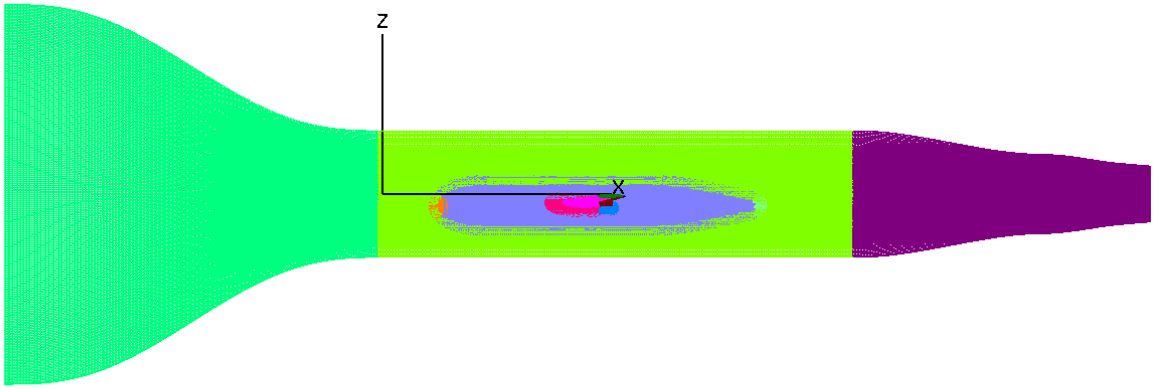

Figure 11. Side view of TC2 with JFM-F6v2 CFD grid, right walls hidden.

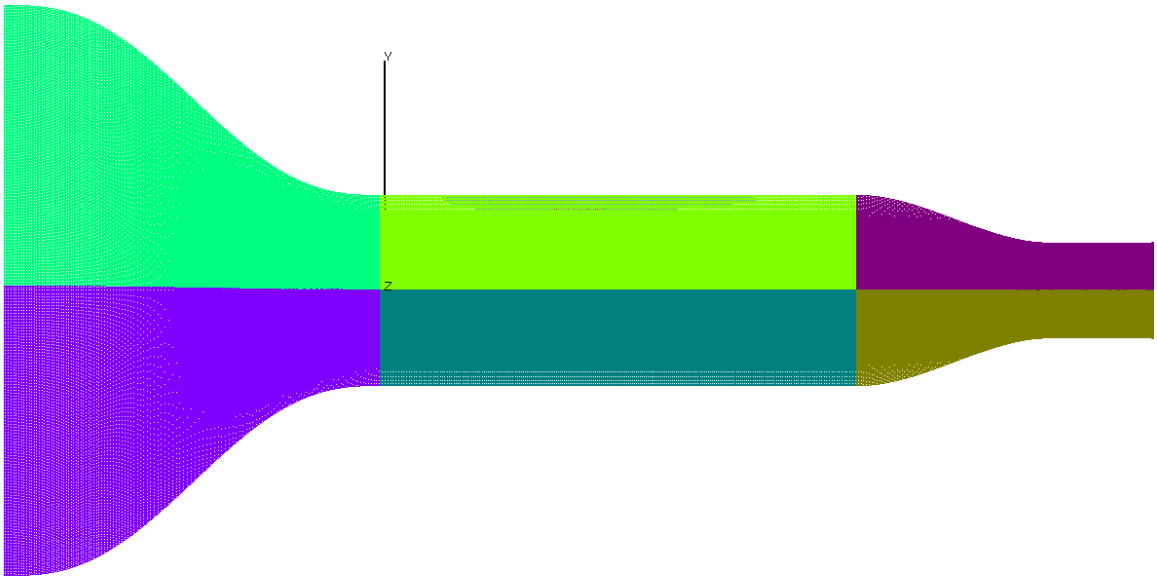

Figure 12. Top view of TC2 with JFM-F6v2 CFD grid.

IV. Results

Comparison of Experimental Fluid Dynamics (EFD) and Computational Fluid Dynamics (CFD)

A full span tunnel-centered model is less challenging to simulate than a wall-mounted model due to the large influence of the incoming wall boundary layer. Techniques including using a peniche or a splitter plate can help the CFD data better correlate with experimental data, but these options are not always available. Nevertheless, in the current experiment, the approach taken was to model the physical experiment as closely as possible, including the influence of the tunnel wall boundary layer, so that differences between EFD and CFD are indicative of either modeling or measurement deficiencies.

Figure 13 depicts the oil flow and the CFD surface streamlines in the juncture flow region. The CFD results show a distinct clear separation bubble, while the oil flow suggests a smaller side of body separation. A distinctive side of body separation was not evident in the EFD.

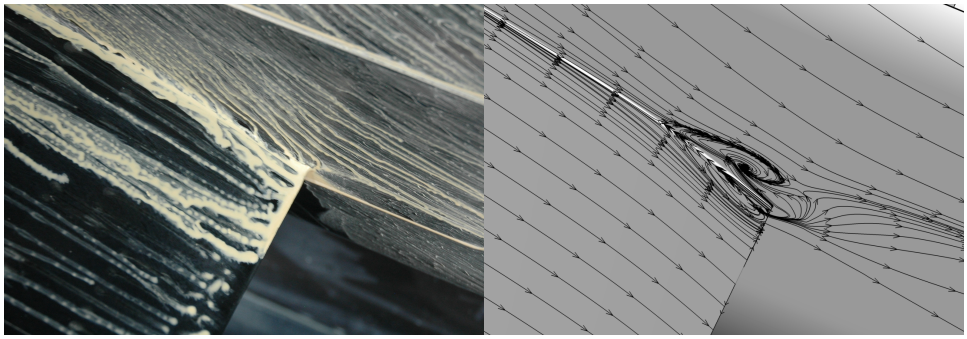

Figure 13. Oil Flow (left) and CFD surface streamlines (right) at the juncture flow region.

Gand *et al.*[7] shows that a thick fuselage boundary layer and a strong horseshoe vortex generated by the wing suppresses the side of body separation. The TC2 experimental results follow this trend. To correctly simulate the juncture flow, both the horseshoe vortex and the wing boundary layer have to be captured accurately. The CFD results show evidence of a thinner boundary layer and a weak horseshoe vortex, leading to a large separation region. Figure 14 from Barber[13] illustrates these results. These statements are supported in the results given below.

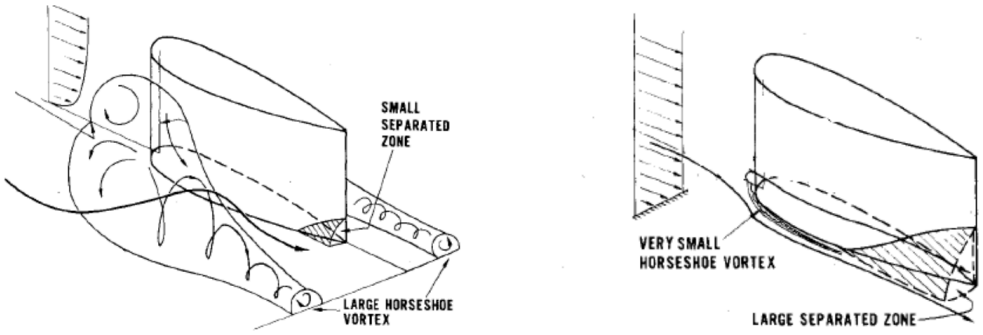

(a) thick boundary layer (b) thin boundary layer

Figure 14. Model proposed by Barber *et al.*[13] for boundary layer/wing interaction.

Boundary layer profiles taken at several different positions along the tunnel wall half-way between the tunnel inlet and the fuselage nose, X = 7.75 inches, and are shown in figure 15a where they are compared with CFD results taken at the same locations. The overall height of the boundary layers at the same position are comparable, but the overall shape is slightly different. This may be caused by minor difference in roughness and steps in the tunnel, which would reduce the experiment's velocity. Note that CFD modeled boundary layer profiles are shown as solid lines, and experimental results are shown as dots.

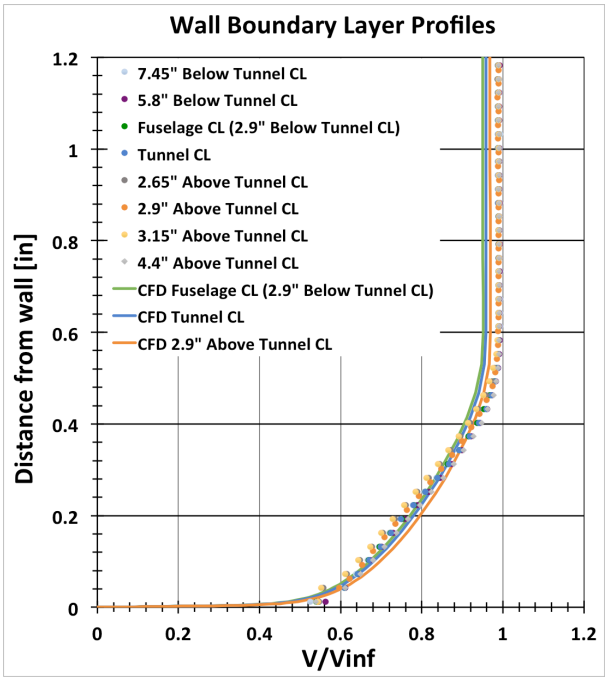

Figure 15a. Tunnel wall BL profile, X= 7.75 inches.

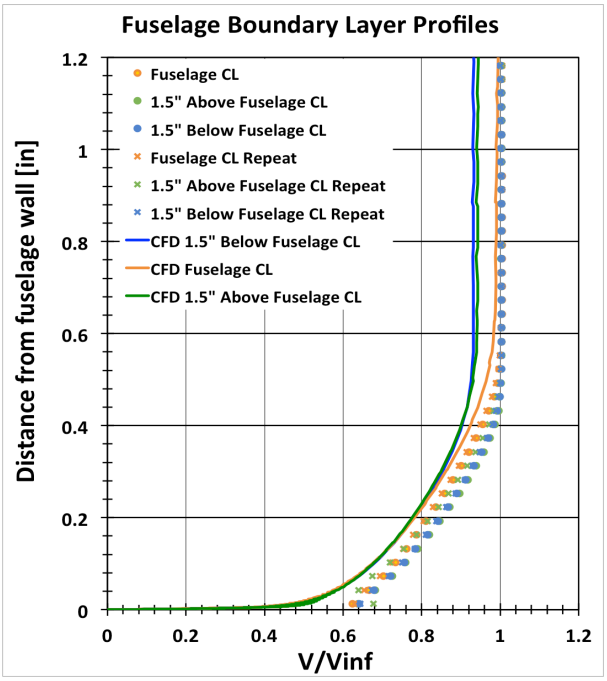

Figure 15b. Fuselage BL profile, X = 41.625 inches.

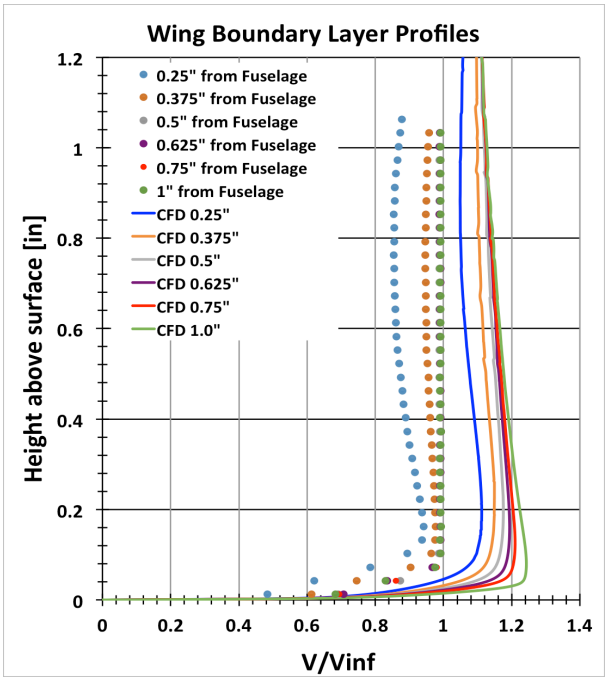

Figure 15c. Wing BL profile, X = 45.75 inches.

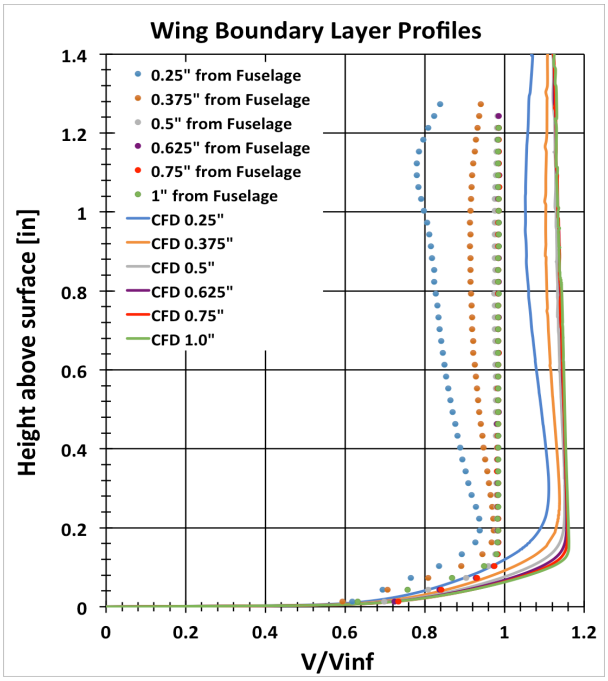

Figure 15d. Wing BL profile, X = 49.75 inches.

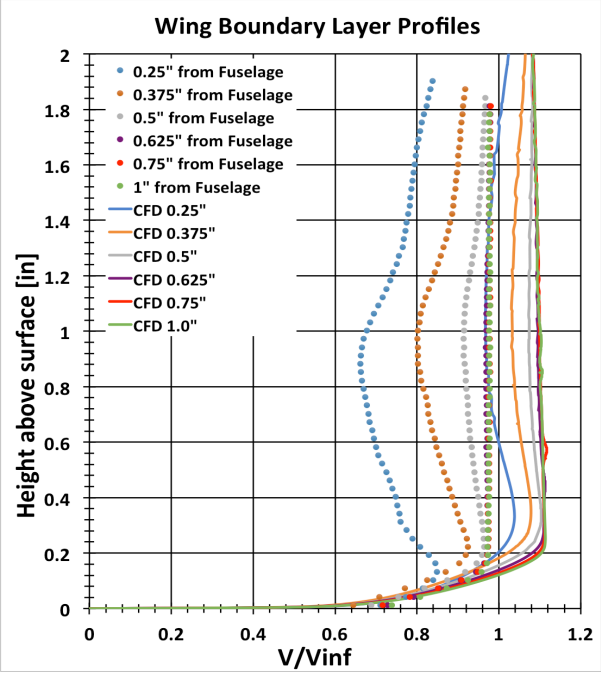

Figure 15e. Wing BL profile, $X = 53.75$ inches.

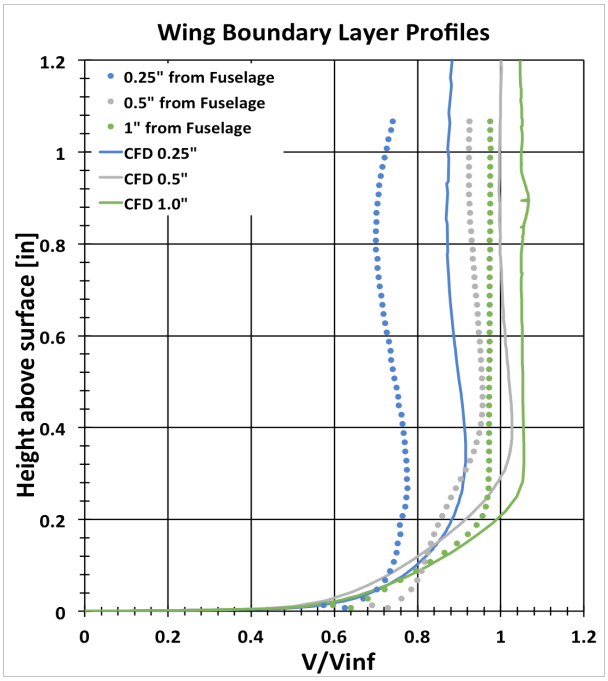

Figure 15f. Wing BL profile, $X = 56.25$ inches.

Figure 15. Experimental and computational boundary layer profiles at different tunnel stations.

The comparison of boundary layer profiles in figures 15a and 15b, which were taken on the wall (X = 7.75 inches) and fuselage upstream of the wing (X = 41.625 inches), shows experimental measurements exhibit a slightly higher velocity than the CFD results. This suggests that the CFD is seeing a stronger influence from the model upstream of the nose and the leading edge of the wing.

Comparing the flow over the wing, experimental data shows a larger influence from the boundary layer on the fuselage than the CFD results show. The CFD data thus suggests a thinner boundary layer on the fuselage, evident in the increased velocities in the wing junction. The boundary layer height on the wings compare fairly well for both EFD and CFD. Figure 15d shows that the EFD boundary layer profile 0.25 inch away from the fuselage wall has a dip in velocity about 1 inch above the wing, suggesting the presence of a horseshoe vortex. This horseshoe vortex is also evident in figure 15e where the EFD BL profiles 0.25 inch and 0.375 inch away from the fuselage and 0.8 inch above the wing show a similar dip. Figure 15f EFD boundary layer profile measured at 0.5 inch away from the fuselage wall exhibits a small dip in velocity at about 0.2 inch above the wing. It's possible that the horseshoe vortex is supressing the boundary layer profile here, causing the abnormal shape. Overall, CFD is computing a velocity increase over the wing, while EFD is showing a larger influence from the boundary layer on the fuselage.

Two pressure probe surveys were conducted looking at the velocity just downstream of the wing trailing edge in the vicinity of the junction at X = 58.75 inches. Figure 16 shows a comparison of the computed and measured normalized velocity survey in a 2 inch square plane (0.1 inch spacing between points), overlaid with a high resolution 0.9 inch square (0.03 inch spacing between points) downstream of the trailing edge. The CFD shows evidence of separation in the low speed region, but the EFD does not. As mentioned previously, the total pressure probe is not as accurate as desired in flows with high angularity, but the measured velocity contours would be lower than the observed 0.4 level if flow reversal was present.

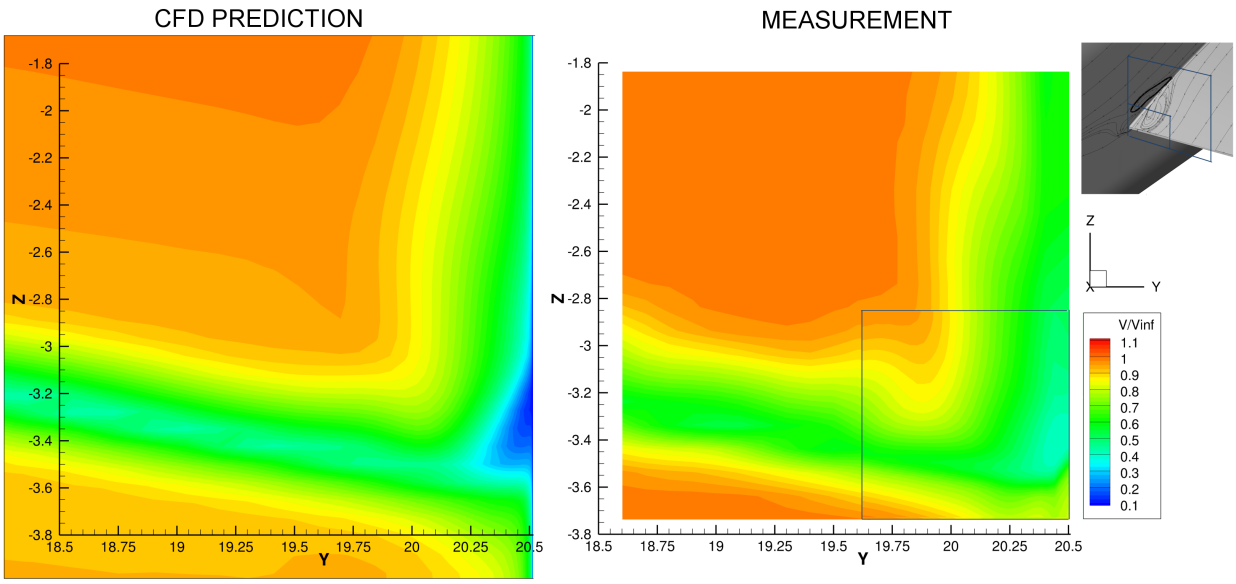

Figure 16. Comparison of measured and computed V/V_∞ just downstream of the trailing edge at X = 58.75 inch with EFD data sampled at every 0.1 inch (inset box sampled every 0.03 inch).

The horseshoe vortex generated by the fuselage is fairly large, and both the experiment and the CFD simulations detect this. The CFD simulations shows the vortex persists along the length of the fuselage on the tunnel as shown in figures 17 and 18. Figure 17 shows the horseshoe vortex formed upstream of the fuselage and uniform streamlines along the fuselage with a slight upwash as the flow approaches the wing. Figure 18 shows a constant x-slice plane colored by Mach contours. The influence of this horseshoe vortex on the wing juncture flow needs further investigation.

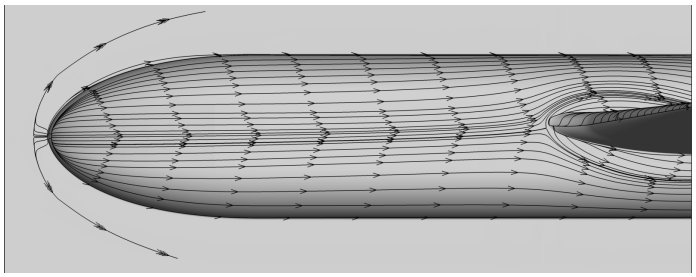

Figure 17. CFD solution, streamlines on fuselage.

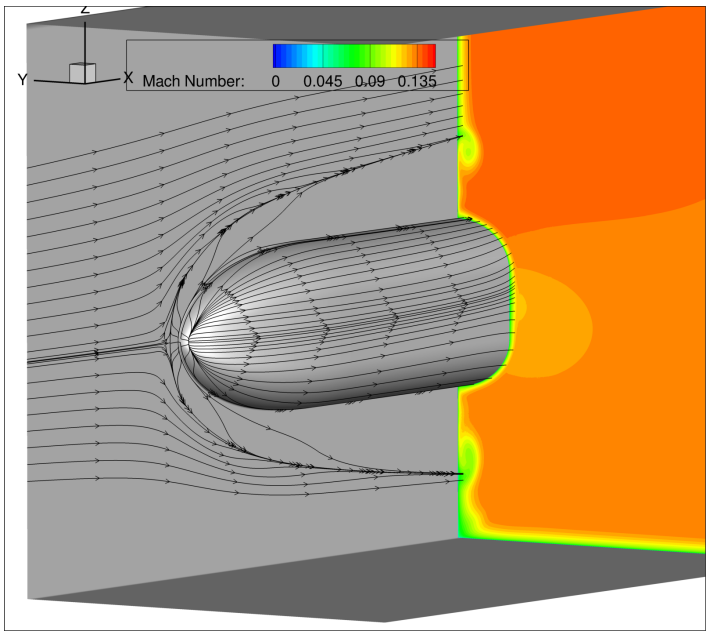

Figure 18. CFD streamlines on fuselage and tunnel wall, with a constant X = 41.625 inches slice colored by Mach contours.

V. Conclusions

The research discussed in this paper focuses on comparing experimental measurements and computational results of the wing-fuselage juncture flow of a representative commercial airline configuration. Flow separation zones of significant extent were not observed in a wind tunnel test of a semi-span version of the JFM (i.e. the JFM F6v2 model with horn) at zero angle of attack; yet, computations of the same flow field show flow separation on the wing and the fuselage in the junction region near the wing trailing edge. The research supports the following conclusions:

1.) To correctly simulate the juncture flow, both the horseshoe vortex and the wing boundary layer must be captured accurately.
   a. The wing horseshoe vortex is much stronger in the EFD than is computed by the CFD.
   b. The stronger horseshoe vortex in the EFD contributes to the lack of separation bubble; however, CFD computes a thinner boundary layer causing a weaker wing vortex, resulting in a larger side-of-body separation.
   c. As shown in boundary layer profiles, the influence of the fuselage boundary layer is very apparent in the EFD but very little influence is seen in the CFD.
2.) CFD sees a more substantial upstream influence of the model than EFD measures.

VI. Acknowledgments

The authors would like to thank the NASA Transformational Tools and Technologies Project for support of the research presented in this paper.

VII. References

[1]Rumsey, Christopher L., Neuharty, Dan H., and Kegerisez, Michael A., "The NASA Juncture Flow Experiment: Goals, Progress, and Preliminary Testing (Invited)," AIAA SciTech Forum, San Diego, CA, January, 2016.

[2]Laflin, K. R., Vassberg, J. C., Wahls, R. A., Morrison, J. H., Brodersen, O., Radowitz, M., Tinoco, E. N., and Godard, J., "Summary of Data from the Second AIAA CFD Drag Prediction Workshop," AIAA Paper 2004-0555, January 2004.

[3]Sclafani, Anthony J., DeHaan, Mark A., Vassberg, John C., Rumsey, Christopher L., and Pulliam, Thomas H., "Drag Prediction for the Common Research Model Using CFL3D and OVERFLOW" Journal of Aircraft, Vol 51, No 4, July-August, 2014 p. 1101-1117.

[4]Spalart, P. R. and Allmaras, S. R., "A One-Equation Turbulence Model for Aerodynamic Flows," *Recherche Aerospatiale*, No. 1, 1994, pp. 5–21.

[5]Zilliac, G.G., Pulliam, T., Rivers, M., Zerr, J., Delgado, M., Halcomb, N and Lee, H., "A Comparison of the Measured and Computed Skin Friction Distribution on the Common Research Model" AIAA paper 2011-1129, AIAA Aerospace Sciences meeting, Orlando, 2011.

[6]Simpson, Roger L., "Junction Flows," Annual Review of Fluid Mechanics, Vol. 33, 2001, pp. 415:443

[7]Gand, Fabien, Deck, Sébastien, Brunet, Vincent and Saguat, Pierre, "Flow Dynamics Past a Simplified Wing Body Junction," Physics of Fluids 22, 2010.

[8]Sclafani, A. J., Vassberg, J. C., Winkler, C., Dorgan, A. J., Mani, M., Olsen, M. E., and Coder, J. G., "Analysis of the Common Research Model Using Structured and Unstructured Mashes," *Journal of Aircraft*, Vol. 51, No. 4, 2014, pp. 1223–1243.

[9]Nichols, R. H. and Buning, P. G., "User's Manual for OVERFLOW 2.2, August 2010," http://people.nas.nasa.gov/~pulliam/Overflow/ Overflow Manuals.html (retrieved Nov. 2015).

[10]Olsen, Michael E., Lillard, Randolph P., and Murman, Scott M., "Prediction of Large Separations with Reynolds Stress Models," AIAA paper 2013-2720, 21st. Computational Fluid Dynamics Conference, San Diego, January 2013.

[11]Spalart, P. R., "Strategies for Turbulence Modelling and Simulation," *International Journal of Heat and Fluid Flow*, Vol. 21, 2000, pp. 252-263.

[12]Chan, W. M., Gomez, R. J., Rogers, S. E. and Buning, P. G., "Best Practices in Overset Grid Generation," AIAA Paper 2002-3191, 32nd AIAA Fluid Dynamics Conference, St. Louis, Missouri, June, 2002 (invited).

[13]Barber, T. J., "An Investigation of Strut-Wall Intersection Losses," Journal of Aircraft, Vol 15, No. 10, 1978, pp. 676-681.